



Research article

Designing and tuning MIMO feedforward controllers using iterated LMI restriction

Saeedreza Tofighi*, Farshad Merrikh-Bayat and Farhad Bayat

Department of Electrical and Computer Engineering, University of Zanjan, University Blvd., Zanjan 45371-38791, Iran

* **Correspondence:** Email: saeedreza.tofighi@znu.ac.ir.

Abstract: In this paper, a multi-input multi-output (MIMO) feedforward control structure is proposed and designed based on the linear matrix inequality (LMI) approach to improve disturbance rejection and reference tracking of the given feedback system. The proposed architecture consists of two MIMO feedforward controllers, where each controller can be designed independently using the proposed method. The unknown variables of the feedforward controllers are calculated using LMI restrictions such that the H_∞ -norm of the transfer function matrix from disturbance (set-point) to output (error) is minimized. By taking advantage of the frequency sampling techniques and using some iterative algorithms, convergence of the solution to a local optimal point is guaranteed. For solving this optimization problem the CVX optimization tool is used and the numerical results are presented. The proposed method can be considered as a new tractable approach for tuning the parameters of MIMO feedforward controllers.

Keywords: MIMO feedforward controller; disturbance rejection; set-point tracking; linear matrix inequality (LMI); semidefinite program (SDP) optimization

1. Introduction

A majority of industrial plants and chemical processes are multivariable. These systems often exhibit strong couplings between apparently non-related inputs and outputs. In this regard, the disturbance rejection and set-point tracking goals are challenging tasks. Although the importance of disturbance rejection is not less than the set-point tracking, in the context of linear MIMO systems it

has gained less attention in the literature.

Designing and exerting a feedforward controller is a possible solution to improve the set-point tracking and disturbance rejection properties of the feedback system. A technique for determination of a feedforward control law to be applied to a closed-loop PID-based control system with a MIMO process in the loop is presented in [1]. Experimental evaluation of feedforward tuning rules is presented in [2]. In [3] a dual-mode adaptive fractional order PI controller with a feedforward controller for quadruple tank process is presented. Disturbance attenuation using feedforward compensation for flight test results is studied in [4], and transient response optimization via feedforward control is proposed in [5]. In [6] comparison of additive and multiplicative feedforward control is presented. Disturbance rejection via feedforward compensation using an enhanced equivalent input disturbance approach is studied in [7]. The iterative tuning of a feedforward controller with disturbance compensator for servo systems is presented in [8]. Feedforward control techniques are also used in industries. For example, a method for MIMO feedforward control of multi-harmonic gearbox vibrations is presented in [9]. In [10] active disturbance rejection control based on feedforward inverse system for turbofan engines is proposed. As another example, feedforward-feedback control of a solid oxide fuel cell power system is presented in [11]. Finally, in [12] a review on industrial feedforward control technology is given.

Linear Matrix Inequalities (LMIs) provide us with a powerful tool to solve a wide variety of optimization and control problems. Designing MIMO controllers, and especially MIMO PIDs, via LMIs had been the subject of many studies; see for example [13–16]. An important advantage of LMIs is that they are convex, and consequently, can be solved very effectively by using commercial software in a polynomial time. Many problems in the field of control theory like stability analysis of linear systems [17], calculating the H_∞ -norm of a transfer function/matrix [18], calculating the upper bound on μ [18] and state-feedback control [19] can be formulated using the LMI approach. There are also many other problems which are non-convex and cannot be represented by LMIs. Hence, a large effort is made to cope with the non-convexity of these problems and finding approximate solutions using LMIs. Convex-concave decomposition and linearization method are proposed in [20] to transform non-convex and bilinear matrix inequalities (BMIs) into LMIs. As an application of such techniques, tuning of MIMO PIDs using the LMI approach is introduced in [15]. The main idea in that paper is to transform a MIMO PID controller design problem to a static output feedback problem whose solution via LMI approach was already known. Another considerable work in this field is [16]. In this paper, the MIMO PID controller is obtained by minimizing the low-frequency gain of the open-loop system subject to constraints on infinity norms of standard closed-loop transfer functions.

In this paper, we describe a method for designing MIMO feedforward controllers. The method is based on solving a small number of convex optimization problems, each one in the form of a semidefinite programming (SDP). The proposed architecture consists of two MIMO feedforward controllers; one from disturbance and the other from set-point to the input of the plant. In order to improve the disturbance rejection of feedback system the unknown variables of the feedforward controllers are calculated using LMIs such that the H_∞ -norm of the transfer matrix from disturbance to the output of plant is minimized. Also, to improve the tracking capability of the feedback system, the transfer matrix from the set-point to error is minimized. The proposed formulation to solve the problem is essentially non-convex and non-linear. By exerting some frequency sampling techniques and using some iterative algorithms such as convex-concave decomposition, a new method is developed to solve the problem. The proposed method is designed in the frequency domain and has an iterative nature

which means that an initial point, which is actually a stable transfer matrix, is required to begin the search. Note that finding a solution, if one exists, is not guaranteed and the resulting solution may be suboptimal. After presenting the theoretical results, some practical examples are presented to show the performance of the proposed feedforward controller design method. Efficiency of the proposed method is also evaluated by employing integral of absolute error (IAE), integral of squared error (ISE), integral of time multiplied by absolute error (ITAE), and integral of time multiplied by squared error (ITSE) performance indices. This method could be extended to non-linear systems using the method proposed in [21]

The rest of this paper is organized as follows. The main results, including the proposed control structure and the proposed algorithm for tuning dual-feedforward MIMO controller using LMIs, is presented in Sections 2–4. Four illustrative examples are presented in Sections 5 and 6 concludes the paper.

2. Statement of the problems

The proposed dual-feedforward architecture for the closed-loop system is shown in Figure 1, where $r(t)$ is the reference input, $e(t)$ is the error, and d is a measurable output-referred plant disturbance. The signals $u(t)$ and $y(t)$ are the plant input and output, respectively.

The plant, denoted as $P(s)$, is linear and time-invariant which has m inputs (actuators) and p outputs (sensors). Also, there are at least as many actuators as plant outputs, which means that $p \leq m$. It is assumed that the controller, $C(s)$, has already been designed using any appropriate method. Of course, this controller must provide internal stability and secures a good set-point tracking performance. It is also desired, but not necessary, that this controller can partly reject disturbances. In this paper, we aim to propose an additional stage to improve disturbance rejection and set-point tracking.

In the following we propose a new structure for the MIMO feedforward controller. For the sake of simplicity and without any loss of generality, we assume that the MIMO plant has two inputs and two outputs. In Figure 1, F_1 and F_2 are the proposed feedforward controllers to be designed. It is also assumed that each entry of these two transfer matrices is a first-order (stable) transfer function. This assumption simplifies the tuning and implementation of the feedforward controllers and also drastically reduces the complexity of computations. Hence, the structure of each of the feedforward controllers in Figure 1 is considered as follows

$$F = WX (WV)^{-1} \quad (1)$$

where W is a matrix weight function in the Laplace variable, s , X is an unstructured matrix variable and V is a structured matrix variable, which are defined as follows

$$W(s) = \begin{bmatrix} s^p \dots s^0 & \mathbf{0}_{1 \times q} & \dots & \mathbf{0}_{1 \times q} \\ \mathbf{0}_{1 \times q} & s^p \dots s^0 & \dots & \vdots \\ \vdots & \dots & \ddots & \mathbf{0}_{1 \times q} \\ \mathbf{0}_{1 \times q} & \dots & \mathbf{0}_{1 \times q} & s^p \dots s^0 \end{bmatrix}, X = \begin{bmatrix} x_{11} & \dots & x_{1 \times n} \\ \vdots & \dots & \vdots \\ x_{q \times 1} & \dots & x_{q \times n} \\ \vdots & \dots & \vdots \\ x_{(mq+1) \times 1} & \dots & x_{(mq+1) \times n} \\ \vdots & \dots & \vdots \\ x_{nq \times 1} & \dots & x_{nq \times n} \end{bmatrix}$$

$$V = \begin{bmatrix} v_{11} & \dots & \mathbf{0}_{1 \times q} \\ \vdots & \dots & \mathbf{0}_{1 \times q} \\ v_{q \times 1} & \dots & \mathbf{0}_{1 \times q} \\ \vdots & \dots & \vdots \\ v_{(q+1) \times 2} & \dots & \vdots \\ \vdots & \dots & \vdots \\ v_{2q \times 2} & \dots & \mathbf{0}_{1 \times q} \\ \vdots & \dots & \mathbf{0}_{1 \times q} \\ \vdots & \dots & v_{(mq+1) \times n} \\ \mathbf{0}_{1 \times q} & \dots & \mathbf{0}_{1 \times q} \\ \vdots & \dots & v_{nq \times n} \end{bmatrix}$$

where p is the order of each entry of the feedforward controller, n is the number of inputs or outputs of the $n \times n$ system matrix, and $q = p + 1$. For a two-input two-output system, the feedforward controller matrices will be as follows

$$W = \begin{bmatrix} s & 1 & 0 & 0 \\ 0 & 0 & s & 1 \end{bmatrix}, X = \begin{bmatrix} x_{11} & x_{12} \\ x_{21} & x_{22} \\ x_{31} & x_{32} \\ x_{41} & x_{42} \end{bmatrix}, V = \begin{bmatrix} v_{11} & 0 \\ v_{21} & 0 \\ 0 & v_{32} \\ 0 & v_{42} \end{bmatrix} \quad (2)$$

The reason for proposing the above structure for both F_1 and F_2 in Figure 1 is that it simplifies the stability analysis of the whole system. More precisely, it can be easily proved that the system shown in Figure 1 remains stable after adding F_1 and F_2 if the original closed-loop system (which consists of $C(s)$ and $P(s)$) is stable before adding these two systems, and F_1 and F_2 are stable and defined as given in (1) and (2).

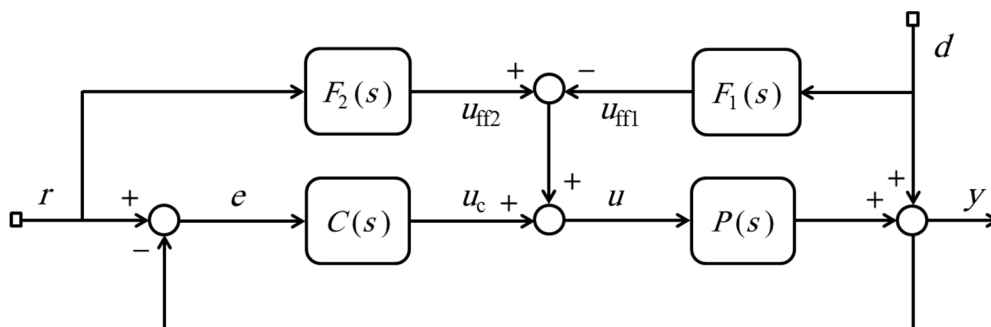


Figure 1. Schematic of the closed-loop system with the proposed feedforward controllers.

For designing a dual-feedforward MIMO controller, the LMI method is employed to calculate the (sub)optimal controllers. In Figure 1 the error is calculated as the following

$$E = -(I + PC)^{-1} (I - PF_2)R + (I + PC)^{-1} (I - PF_1)D \quad (3)$$

where $S = (I + PC)^{-1}$ is the *sensitivity function*. According to Eq (3), for disturbance rejection we need to minimize $\bar{\sigma}[S(I - PF_1)]$. Also, to improve set-point tracking we should minimize $\bar{\sigma}[S(I - PF_2)]$. Hence, F_1 and F_2 are mainly responsible to improve disturbance rejection and set-point tracking, respectively. For the sake of clarity, these two objectives are discussed in two separate sections in the following.

3. Disturbance rejection problem: Theorem, proof, and controller design algorithm

The procedure of designing the feedforward controller F_1 to improve disturbance rejection is considered here. Therefore, the following theorem is performed to obtain the F_1 parameters.

Theorem 1: A sufficient condition to obtain the values of the feedforward controller parameters $F_1(s)$ to improve the disturbance rejection time is obtained by solving the following optimization problem.

$$\min t \quad (4.a)$$

$$s.t. \quad \Phi_1 \preceq t \quad (4.b)$$

$$\Phi_3 \preceq 0, \quad k = 1, \dots, N \quad (4.c)$$

where, Φ_1 and Φ_3 are introduced in the rest of this section.

Proof: As mentioned earlier, for this purpose we should minimize $\bar{\sigma}[S(I - PF_1)]$. the design problem is formulated as follows

$$\min t \quad (5.a)$$

$$s.t. \quad \bar{\sigma} \left[(I + P(0)K_f)^{-1} (I - P(0)W(0)X_1 (W(0)V_1)^{-1}) \right] \leq t \quad (5.b)$$

$$\bar{\sigma} \left[S (I - PWX_1 (WV_1)^{-1}) \right] \leq S_{\max}, \quad \forall \omega \quad (5.c)$$

Note that since the energy of disturbance is mainly concentrated at low frequencies, Eqs (5.a) and (5.b) minimize the singular value of the corresponding transfer matrix at zero frequency. On the other hand, it is a well-known fact that minimizing the sensitivity function, S , at low frequencies leads to increasing the peak of S at higher frequencies, which is not desired. So, the constraint in (5.c) is taken into account to make sure that the resulting control system has a good stability margin and the overshoots in the step response do not exceed the specified amount. Reasonable values of S_{\max} are in the range of 1.1 to 1.6; this is for sensitivity and complementary sensitivity peaking constraint in our design problem, lower values give a more damped closed-loop system.

Finding a solution to the optimization problem in (5) is not straightforward since (5.b) and (5.c) are not linear in the unknown matrices X and V containing the coefficients of controllers. Hence, an approximate method to find a (sub)optimal solution to this problem is developed in the following.

Consider $\bar{\sigma} \left[S (I - PWX_1 (WV_1)^{-1}) \right] \leq S_{\max}$ for all ω 's as given in (5.c). Since the frequency can take all values greater than or equal to zero, this statement actually consists of an infinite number of

constraints, and for this reason it is called a semi-infinite constraint. A Semi-infinite constraint can be handled by replacing it with a finite set of constraints obtained by evaluating the frequency-dependent function at given frequencies. For example, we use $\bar{\sigma}[S(i\omega_k)] \leq S_{max}$, $k = 1, \dots, N$ instead of the constraint $\|S\|_{\infty} \leq S_{max}$ in Eq (5.b). For the sake of simplicity in notation, in the following we will use subscripts to denote a transfer matrix evaluated at the frequency $s = i\omega_k$. For example, for a given complex matrix, the notation $P_k = P(i\omega_k)$ is used. The sampled problem is then obtained in the following form,

$$\min t \quad (6.a)$$

$$s.t. \quad \bar{\sigma} \left[(I + P(0)K_f)^{-1} (I - P(0)W(0)X_1 (W(0)V_1)^{-1}) \right] \leq t \quad (6.b)$$

$$\bar{\sigma} \left[S_k (I - P_k W_k X_1 (W_k V_1)^{-1}) \right] \leq S_{max}, \quad k = 1, \dots, N \quad (6.c)$$

Now, in order to convert the above sampled problem into LMI form, we need to eliminate the non-linearity from it.

In order to represent the constraint in Eq (6.b) in the form of an LMI write it as follows

$$\bar{\sigma} \left[(I + P(0)K_f)^{-1} (W(0)V_1 - P(0)W(0)X_1) (W(0)V_1)^{-1} \right] \leq t \quad (7)$$

Or equivalently,

$$\begin{aligned} \{S(W(0)V_1 - P(0)W(0)X_1)\} \{ (W(0)V_1)^{-1} (W(0)V_1)^{-*} \} \\ \{ (W(0)V_1 - P(0)W(0)X_1)^* S^* \} \preceq t^2 I, \end{aligned} \quad (8)$$

where for a complex matrix $Z \in C^{p \times q}$, Z^* is its (hermitian) conjugate transpose. We used the notation $Z^{-*} = (Z^*)^{-1}$. The matrix inequality symbol $Z \preceq 0$ means that Z is Hermitian and negative semidefinite. Define $Z_1 = S(W(0)V_1 - P(0)W(0)X_1)$ and $A_1 = -(W(0)V_1)^{-1} (W(0)V_1)^{-*}$. Now, rearranging Eq (8) yields

$$-t^2 I - Z_1 (-A_1) Z_1^* \preceq 0 \quad (9)$$

Using Schur complement lemma it is concluded from Eq (9) that

$$\left[\begin{array}{c|c} -t^2 I & Z_1 \\ \hline Z_1^* & A_1^{-1} \end{array} \right] \preceq 0 \quad (10)$$

or equivalently

$$\left[\begin{array}{c|c} -t^2 I & S(W(0)V_1 - P(0)W(0)X_1) \\ \hline (W(0)V_1 - P(0)W(0)X_1)^* S^* & -(W(0)V_1)^* (W(0)V_1) \end{array} \right] \preceq 0 \quad (11)$$

Note that the term $(W(0)V_1)^*(W(0)V_1)$ in Eq (11) is non-linear in variables. To remove this difficulty, first we write Eq (11) as follows

$$\left[\begin{array}{c|c} -t^2 I & S(W(0)V_1 - P(0)W(0)X_1) \\ \hline (W(0)V_1 - P(0)W(0)X_1)^* S^* & 0 \end{array} \right] \preceq \left[\begin{array}{c|c} 0 & 0 \\ \hline 0 & (W(0)V_1)^*(W(0)V_1) \end{array} \right], \quad (12)$$

Now, according to the approximate linearization of quadratic matrix inequalities (QMI) from [16] we can write $(W(0)V_1)^*(W(0)V_1) \geq (W(0)V_1)^*(W(0)\tilde{V}_1) + (W(0)\tilde{V}_1)^*(W(0)V_1) - (W(0)\tilde{V}_1)^*(W(0)\tilde{V}_1)$ where \tilde{V}_1 is an arbitrary matrix of suitable dimension. Applying it to Eq (12) turns out

$$\Phi_1 = \left[\begin{array}{c|c} -t^2 I & S(W(0)V_1 - P(0)W(0)X_1) \\ \hline (W(0)V_1 - P(0)W(0)X_1)^* S^* & \begin{array}{l} -[(W(0)V_1)^*(W(0)\tilde{V}_1) \\ + (W(0)\tilde{V}_1)^*(W(0)V_1) \\ - (W(0)\tilde{V}_1)^*(W(0)\tilde{V}_1)] \end{array} \end{array} \right] \preceq 0 \quad (13)$$

The constraint in Eq (13) is in the form of an LMI. Because Φ_1 is real-valued and does not have an imaginary part, we can use it directly for problem solving.

The constraint in Eq (6.c) can be represented in the form of LMIs by following similar steps. More precisely, rearranging Eq (6.c) yields

$$\bar{\sigma} \left[S(WV_1 - PWX_1)(WV_1)^{-1} \right] \leq S_{max} \quad (14)$$

which turns out

$$\{S(WV_1 - PWX_1)\} \{ (WV_1)^{-1} (WV_1)^{-*} \} \{ (WV_1 - PWX_1)^* S^* \} \preceq S_{max}^2 I \quad (15)$$

Define $Z_2 = S(WV_1 - PWX_1)$ and $A_2 = -(WV_1)^{-1} (WV_1)^{-*}$. Using these new variables Eq (15) results in the following

$$-S_{max}^2 I - Z_2(-A_2)Z_2^* \preceq 0 \quad (16)$$

which using Schur complement lemma can be written as

$$\left[\begin{array}{c|c} -S_{max}^2 I & Z_2 \\ \hline Z_2^* & A_2^{-1} \end{array} \right] \preceq 0 \quad (17)$$

or equivalently

$$\left[\begin{array}{c|c} -S_{max}^2 I & S(WV_1 - PWX_1) \\ \hline (WV_1 - PWX_1)^* S^* & -(WV_1)^*(WV_1) \end{array} \right] \preceq 0 \quad (18)$$

In order to get rid of the nonlinear term $(WV_1)^*(WV_1)$ in Eq (18) first we rearrange it as follows

$$\left[\begin{array}{c|c} -S_{max}^2 I & S(WV_1 - PWX_1) \\ \hline (WV_1 - PWX_1)^* S^* & 0 \end{array} \right] \preceq \left[\begin{array}{c|c} 0 & 0 \\ \hline 0 & (WV_1)^* (WV_1) \end{array} \right] \quad (19)$$

by applying the matrix inequality $(WV_1)^* (WV_1) \succeq (WV_1)^* (W\tilde{V}_1) + (W\tilde{V}_1)^* (WV_1) - (W\tilde{V}_1)^* (W\tilde{V}_1)$ to Eq (19) the following LMI is obtained

$$\Phi_2 = \left[\begin{array}{c|c} -S_{max}^2 I & S(WV_1 - PWX_1) \\ \hline (WV_1 - PWX_1)^* S^* & \begin{array}{c} -[(WV_1)^* (W\tilde{V}_1) \\ + (W\tilde{V}_1)^* (WV_1) \\ - (W\tilde{V}_1)^* (W\tilde{V}_1)] \end{array} \end{array} \right] \preceq 0 \quad (20)$$

Since Eq (20) has imaginary terms, we use the following equivalent real-valued form for problem solving

$$\Phi_3 = \left[\begin{array}{c|c} re(\Phi_2) & im(\Phi_2) \\ \hline -im(\Phi_2) & re(\Phi_2) \end{array} \right] \preceq 0 \quad (21)$$

To summarize the results, the optimization problem described through Eq (6) with some conservativity can be written as Theorem 1.

The above optimization problem can be used in practice to find the unknown parameters of the optimal feedforward controller F_1 which improves the disturbance rejection of system.

4. Set-point tracking problem: Theorem, proof, and controller design algorithm

The feedforward controller F_2 is considered to improve set-point tracking. As mentioned before, according to Eq (3) we should minimize $\bar{\sigma}[S(I - PF_2)]$ to improve tracking property. Therefore, unknown parameters of F_2 can be obtained by solving the optimization problem in Theorem 2.

Theorem 2: A sufficient condition to obtain the values of the feedforward controller parameters $F_2(s)$ to improve the set-point tracking is obtained by solving the following optimization problem.

$$\min t \quad (22.a)$$

$$s.t. \quad \Phi_4 \preceq t \quad (22.b)$$

$$\Phi_k \preceq 0, \quad k = 1, \dots, N \quad (22.c)$$

Proof: Because the structure of both feedforward controllers is similar, the procedure of designing the feedforward controller F_2 is analogous to the designing of F_1 . More precisely, the corresponding LMI constraints are obtained as follows

$$\Phi_4 = \left[\begin{array}{c|c} -t^2 I & S(W(0)V_2 - P(0)W(0)X_2) \\ \hline (W(0)V_2 - P(0)W(0)X_2)^* S^* & \begin{array}{c} -[(W(0)V_2)^* (W(0)\tilde{V}_2) \\ + (W(0)\tilde{V}_2)^* (W(0)V_2) \\ - (W(0)\tilde{V}_2)^* (W(0)\tilde{V}_2)] \end{array} \end{array} \right] \preceq 0 \quad (23)$$

$$\Phi_5 = \left[\begin{array}{c|c} -S_{max}^2 I & S(WV_2 - PWX_2) \\ \hline (WV_2 - PWX_2)^* S^* & \begin{array}{l} -[(WV_2)^*(W\tilde{V}_2)] \\ + (W\tilde{V}_2)^*(WV_2) \\ - (W\tilde{V}_2)^*(W\tilde{V}_2) \end{array} \end{array} \right] \preceq 0 \quad (24)$$

Again, since Eq (24) has an imaginary part, we use the real-valued LMI in (25) instead of that

$$\Phi_6 = \left[\begin{array}{c|c} \text{re}(\Phi_5) & \text{im}(\Phi_5) \\ \hline -\text{im}(\Phi_5) & \text{re}(\Phi_5) \end{array} \right] \preceq 0 \quad (25)$$

hence, according to Eqs (23) and (25) the optimization problem in Eq (6) can be restated (with some conservativity) in the LMI form of Theorem 2.

It is worth saying that due to choosing the same structure for both feedforward controllers F_1 and F_2 , and also considering the fact that the objectives of designing both feedforward controllers are similar to each other, the resulting controllers F_1 and F_2 will also be equal.

5. Numerical examples

In this section, three numerical examples are presented to show the efficiency of the proposed dual-feedforward controller design method to improve the disturbance rejection and set-point tracking. The computations were carried out using the Matlab-based convex modeling framework CVX [22] using the SDPT3 4.0 software [23] for solving the semidefinite program (SDP).

Example 1: The plant considered here is a simplified model of the classic two-input two-output Wood-Berry binary distillation column described in [24]. The plant transfer matrix is in the following form,

$$P_1(s) = \begin{bmatrix} \frac{12.8}{16.7s+1} & \frac{-18.9}{21s+1} \\ \frac{6.6}{10.9s+1} & \frac{-19.4}{14.2s+1} \end{bmatrix} \quad (26)$$

Each entry in this plant is a first-order transfer function. The dynamics are quite coupled, so finding a good MIMO PID controller is not simple. The main controller used here is a PID controller obtained in the following form using the method proposed in [16],

$$K_p = \begin{bmatrix} 0.4401 & -0.4787 \\ 0.2105 & -0.2829 \end{bmatrix}, K_i = \begin{bmatrix} 0.0099 & -0.0097 \\ 0.0031 & -0.0068 \end{bmatrix}, K_d = \begin{bmatrix} -0.0007 & 0.0058 \\ 0.0005 & -0.0040 \end{bmatrix} \quad (27)$$

By considering the above PID controller, the transfer matrix of dual-feedforward MIMO controllers using the proposed LMI approach is obtained as follows

$$F_1(s) = F_2(s) = \begin{bmatrix} \frac{19.72s + 0.9617}{s + 6.126} & \frac{-10.62s - 0.8911}{s + 5.826} \\ \frac{9.019s + 0.3272}{s + 6.126} & \frac{-9.022s - 0.3272}{s + 5.826} \end{bmatrix} \quad (28)$$

Figure 2 shows the simulation results with and without using the proposed feedforward controllers. As it is seen, disturbance rejection and tracking are significantly improved by using the proposed feedforward controllers. In this figure, the complementary sensitivity function is $T = (I + PC)^{-1} PC$. It is the closed-loop transfer function from r to y . Also, control signals are derived in Figure 3. In this figure, Q -parameter defined as $Q = (I + PC)^{-1} C$, is the transfer function from r to u . Its size is a measure of the actuator effort. Moreover, in order to make a more accurate comparison, various performance indices are also calculated and the results are summarized in Tables 1 and 2. The results of Tables 1 and 2 clearly verify the efficiency of the proposed feedforward controllers to improve the performance of the control system.

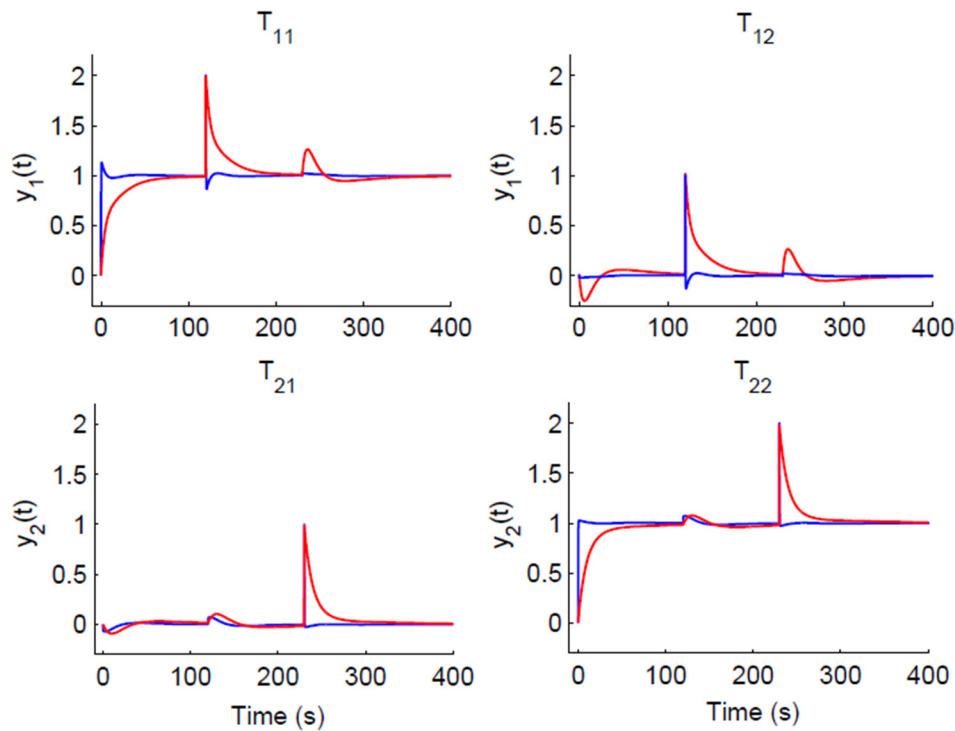


Figure 2. Closed-loop step responses without (red line) and with (blue line) employing the feedforward controllers.

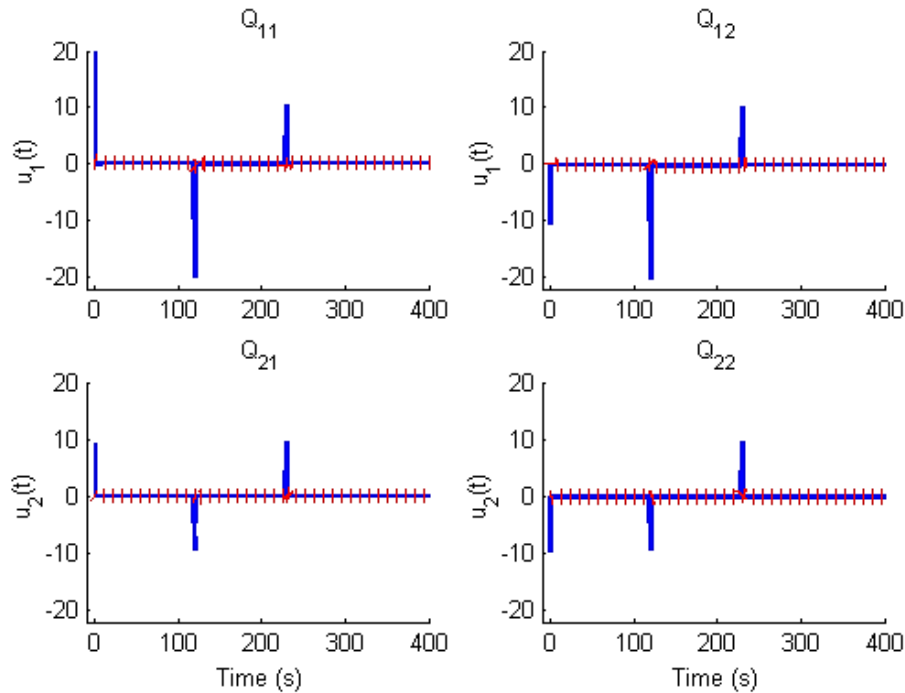


Figure 3. Control signals without (red line) and with (blue line) employing the feedforward controllers.

Table 1. Closed-loop performance indices for disturbance rejection, corresponding to Example 1.

System	Error	IAE	ISE	ITAE	ITSE
With Feedforward	e_1	1.87	0.11	3.74×10^2	0.2104×10^4
Without Feedforward	e_1	21.38	5.98	39.88×10^2	13.775×10^4
With Feedforward	e_2	2.15	0.13	3.77×10^2	0.5442×10^4
Without Feedforward	e_2	16.96	5.30	40.07×10^2	29.156×10^4

Table 2. Closed-loop performance indices for set-point tracking, corresponding to Example 1.

System	Error	IAE	ISE	ITAE	ITSE
With Feedforward	e_1	1.03	0.103	19.66	4.25
Without Feedforward	e_1	14.11	5.131	310.18	969.7
With Feedforward	e_2	0.75	0.77×10^{-2}	33.21	11.39
Without Feedforward	e_2	7.04	80.81×10^{-2}	269.28	694.61

Example 2: The following transfer matrix was proposed in [25] as a benchmark system whose appropriate input-output pairing cannot be determined effectively using the Relative Gain Array (RGA):

$$P_2(s) = \frac{1-s}{(5s+1)^2} \begin{bmatrix} 1 & -4.19 & -25.96 \\ 6.19 & 1 & -25.96 \\ 1 & 1 & 1 \end{bmatrix} \quad (29)$$

This transfer matrix has three non-minimum phase transmission zeros at $s = 1$. The gains of the

MIMO PI controller are obtained as follows [26]

$$K_p = \begin{bmatrix} 0.0821 & 0.0260 & 0.6753 \\ -0.2996 & 0.2071 & -0.6095 \\ 0.0211 & -0.0601 & 0.2449 \end{bmatrix}, K_i = \begin{bmatrix} 0.0022 & 0.0012 & 0.0302 \\ -0.0136 & 0.0099 & -0.0252 \\ 0.0002 & -0.0003 & 0.0021 \end{bmatrix} \quad (30)$$

Assuming the above PI controller in the loop and considering the initial condition as follows

$$\tilde{y} = \begin{bmatrix} 1 & 0 & 0 \\ 1 & 0 & 0 \\ 0 & 1 & 0 \\ 0 & 1 & 0 \\ 0 & 0 & 1 \\ 0 & 0 & 1 \end{bmatrix} \quad (31)$$

The proposed design procedure results in the following feedforward MIMO controllers

$$F_1(s) = F_2(s) = \begin{bmatrix} \frac{1.789s + 4.679}{s + 4.675} & \frac{4.289s - 3.785}{s + 4.683} & \frac{-36.68s + 9.713}{s + 1.942} \\ \frac{20.75s - 5.58}{s + 4.675} & \frac{-28.54s + 4.687}{s + 4.683} & \frac{31.05s - 9.713}{s + 1.942} \\ \frac{1.468s + 0.9008}{s + 4.675} & \frac{4.988s - 0.9023}{s + 4.683} & \frac{-7.159s + 1.942}{s + 1.942} \end{bmatrix} \quad (32)$$

As it could be observed in Figure 4, disturbance rejection and set-point tracking are improved by exerting the feedforward controllers. In this figure, the closed-loop step response of the system with and without the dual-feedforward MIMO method is considered. Also, the results of Tables 3 and 4 show the efficiency of the proposed method by considering different performance indicators for each channel separately. The results of Table 3 confirm that our method acts well for disturbance rejection. Also, the results of Table 4 verify that this method can improve the set-point tracking.

Figure 5 shows the disturbance rejection property of each channel separately with and without feedforward controllers. Also, the disturbance rejection property of the proposed method for three different feedforward controllers obtained by using three different initial conditions is shown in Figure 6. In this figure the blue, black and red plots correspond to the controllers obtained by using the initial conditions $\tilde{y}_1 = 1\tilde{y}$, $\tilde{y}_2 = 5\tilde{y}$ and $\tilde{y}_3 = 10\tilde{y}$ respectively. Also, control signals are derived in Figure 7. The results show that our proposed method converges with different initial conditions and it is not very sensitive to the initial condition used for controller design.

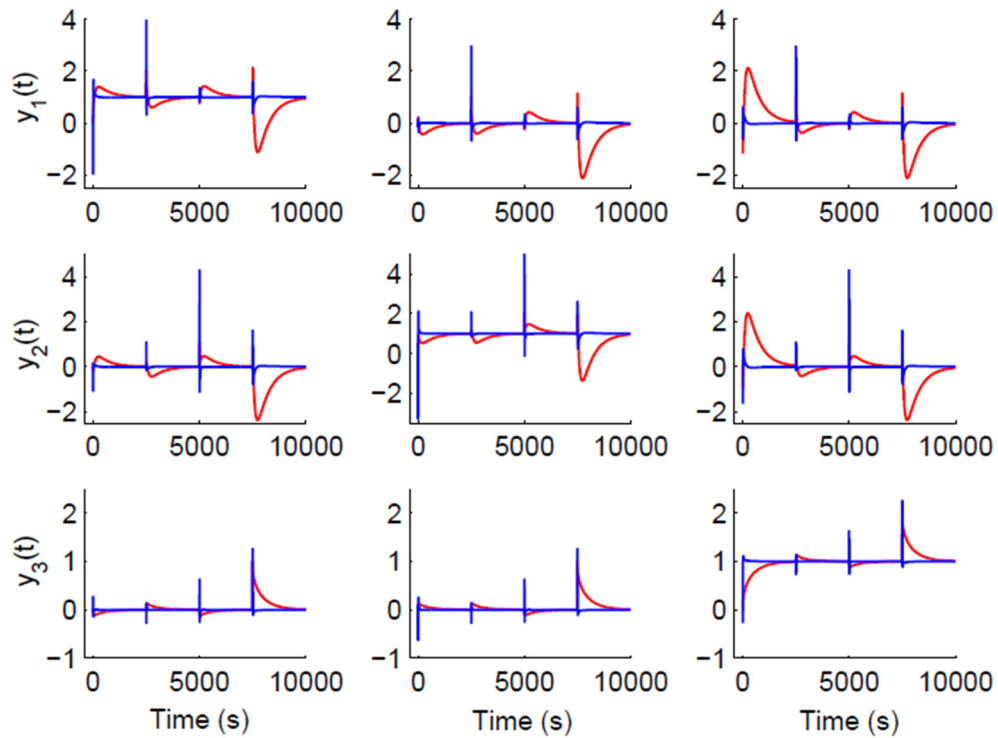


Figure 4. Closed-loop step responses without (red line) and with (blue line) employing the feedforward controllers.

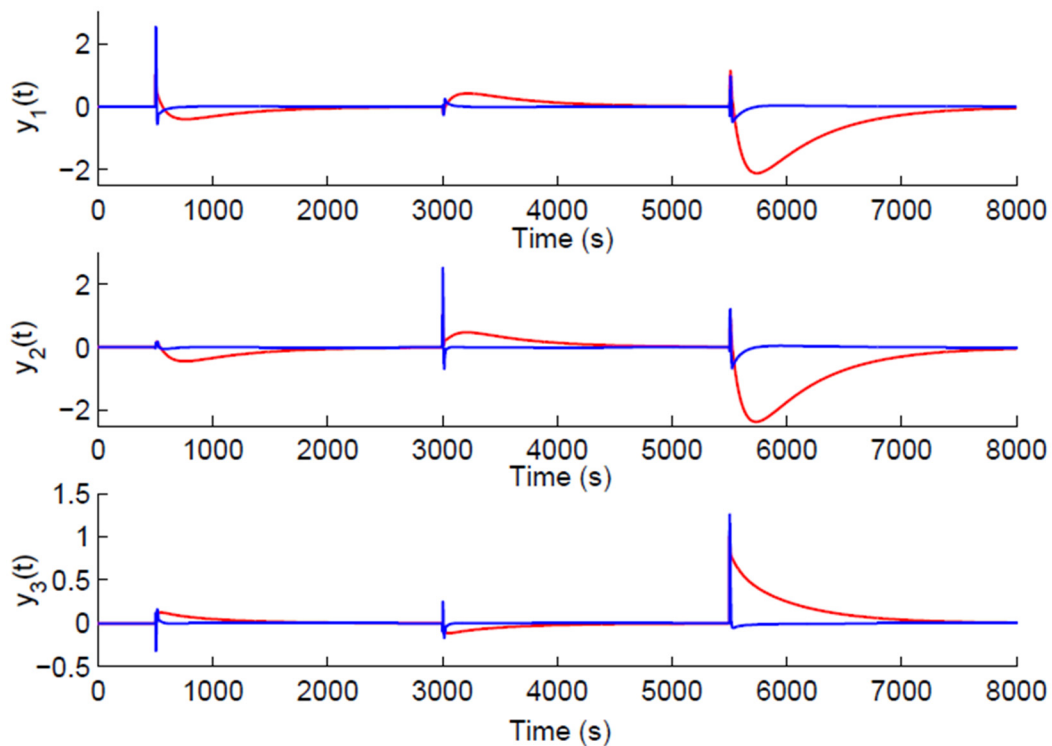


Figure 5. Disturbance rejection property of the MIMO system without (red line) and with (blue line) feedforward controllers.

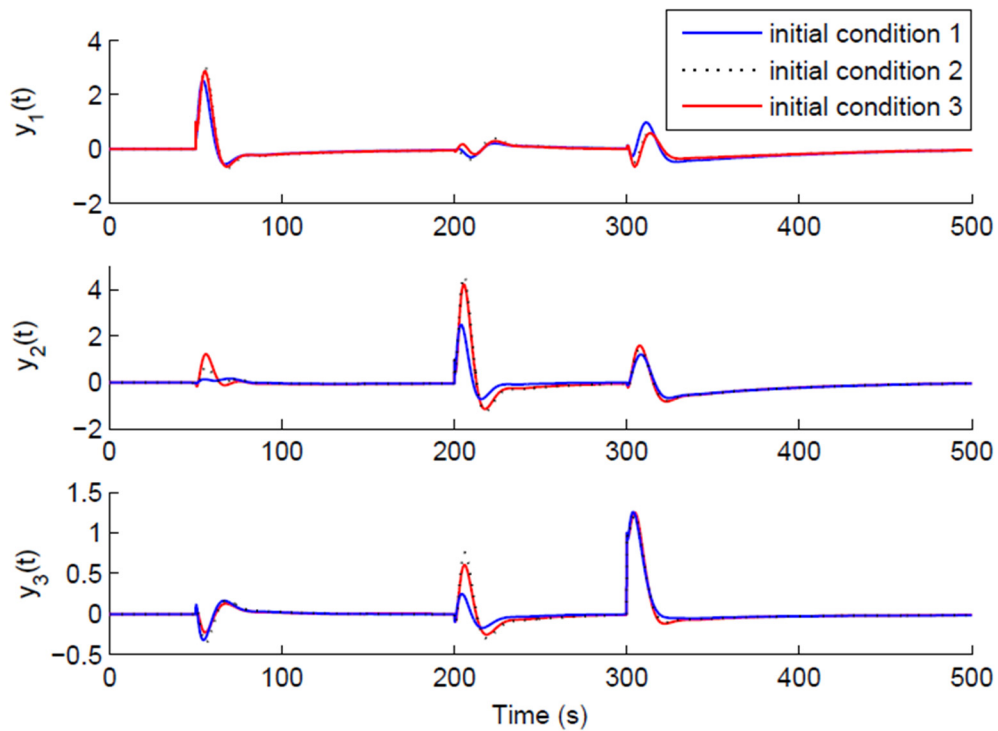


Figure 6. Disturbance rejection of the system with the feedforward controllers designed using three different initial conditions.

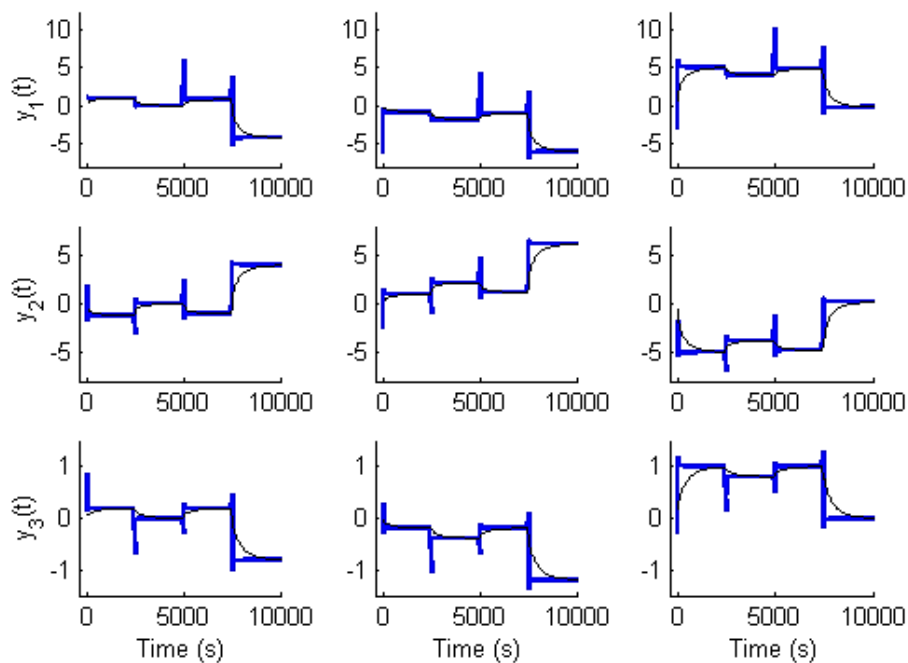


Figure 7. Control signals without (black line) and with (blue line) employing the feedforward controllers.

Table 3. Closed-loop performance indices for disturbance rejection, corresponding to Example 2.

System	Error	IAE	ISE	ITAE	ITSE
With Feedforward	e_1	140.5184	58.8827	0.55066×10^6	0.58806×10^9
Without Feedforward	e_1	2374.9542	2420.2779	12.075×10^6	80.517×10^9
With Feedforward	e_2	138.382	63.212	0.65078×10^6	1.174×10^9
Without Feedforward	e_2	2645.4945	3017.8395	13.483×10^6	100.41×10^9
With Feedforward	e_3	36.5764	13.1393	0.1624×10^6	0.36435×10^9
Without Feedforward	e_3	495.0434	139.6994	2.467×10^6	4.374×10^9

Table 4. Closed-loop performance indices for set-point tracking, corresponding to Example 2.

System	Error	IAE	ISE	ITAE	ITSE
With Feedforward	e_1	88.8646	53.3364	0.02418×10^6	0.003082×10^8
Without Feedforward	e_1	1698.543	2212.4761	1.1051×10^6	6.3458×10^8
With Feedforward	e_2	152.0961	313.5495	0.027849×10^6	0.004313×10^8
Without Feedforward	e_2	1889.8633	2752.8211	1.2242×10^6	7.7752×10^8
With Feedforward	e_3	29.626	18.9988	0.04432×10^6	0.010579×10^6
Without Feedforward	e_3	363.2509	133.7078	1.8214×10^6	16.722×10^6

Example 3: The transfer function matrix of an NMP MIMO system is given as follows [27],

$$P_3(s) = \begin{bmatrix} \frac{-0.495s + 1}{0.08118s^2 + 0.659s + 1} & \frac{0.5(-0.495s + 1)}{0.08118s^2 + 0.659s + 1} \\ \frac{0.5(-1.98s + 1)}{0.3247s^2 + 2.144s + 1} & \frac{-0.495s + 1}{0.08118s^2 + 0.659s + 1} \end{bmatrix} \quad (33)$$

Each entry of the transfer matrix is a second-order transfer function and its dynamics is quite coupled. The feedback controller is a PID controller and the matrix gains of the controller are obtained as the following

$$K_p = \begin{bmatrix} 0.3380 & -0.2459 \\ -0.4355 & 0.2454 \end{bmatrix}, K_i = \begin{bmatrix} 0.0480 & 0.0271 \\ 0.0272 & 0.0479 \end{bmatrix}, K_d = \begin{bmatrix} 0.0093 & -0.0129 \\ 0.0040 & -0.0011 \end{bmatrix} \quad (34)$$

The following dual-feedforward controller is also obtained using the proposed method

$$F_1(s) = F_2(s) = \begin{bmatrix} \frac{-0.1617s + 1.006}{s + 0.7548} & \frac{-0.1024s - 0.6493}{s + 0.974} \\ \frac{0.6174s - 0.5032}{s + 0.7548} & \frac{0.03906s + 1.299}{s + 0.974} \end{bmatrix} \quad (35)$$

The step responses are shown in Figures 8 and 9, respectively. The corresponding ISE performance indices are shown in Figures 10 and 11. These results confirm that the feedforward method acts satisfactorily in improving the disturbance rejection and set-point tracking of the NMP MIMO system.

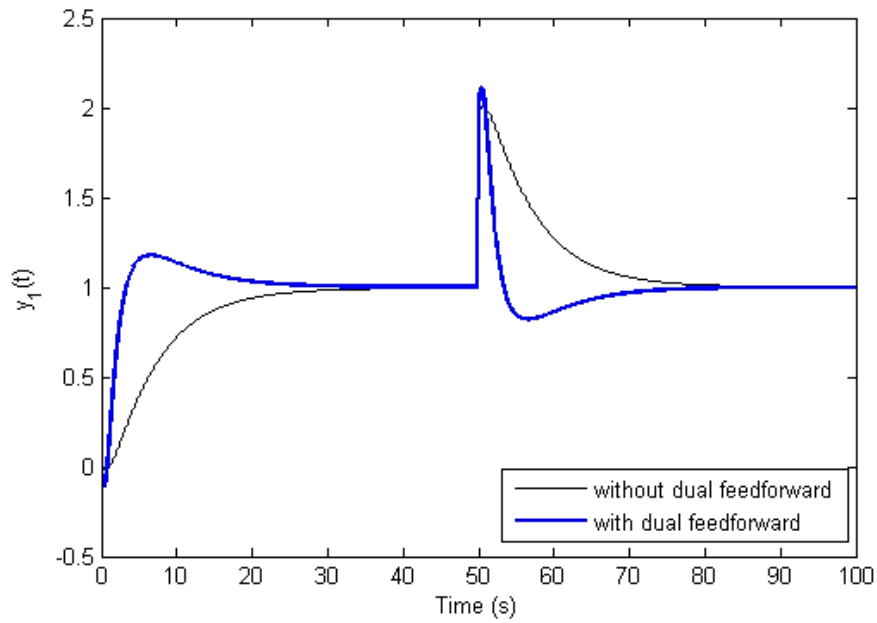


Figure 8. Comparing the closed-loop step response without (black line) and with (blue line) feedforward controller for channel 1.

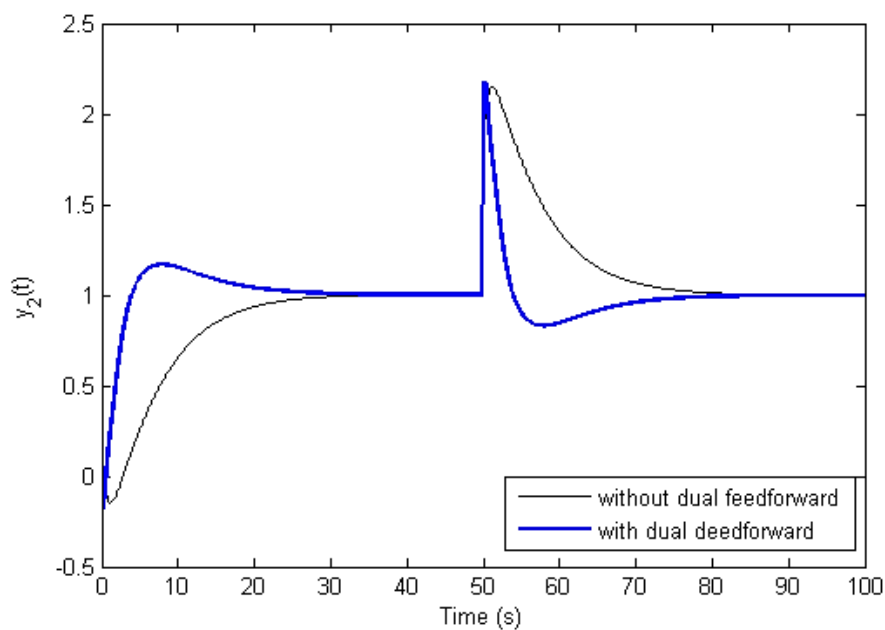


Figure 9. Comparing the closed-loop step response without (black line) and with (blue line) feedforward controller for channel 2.

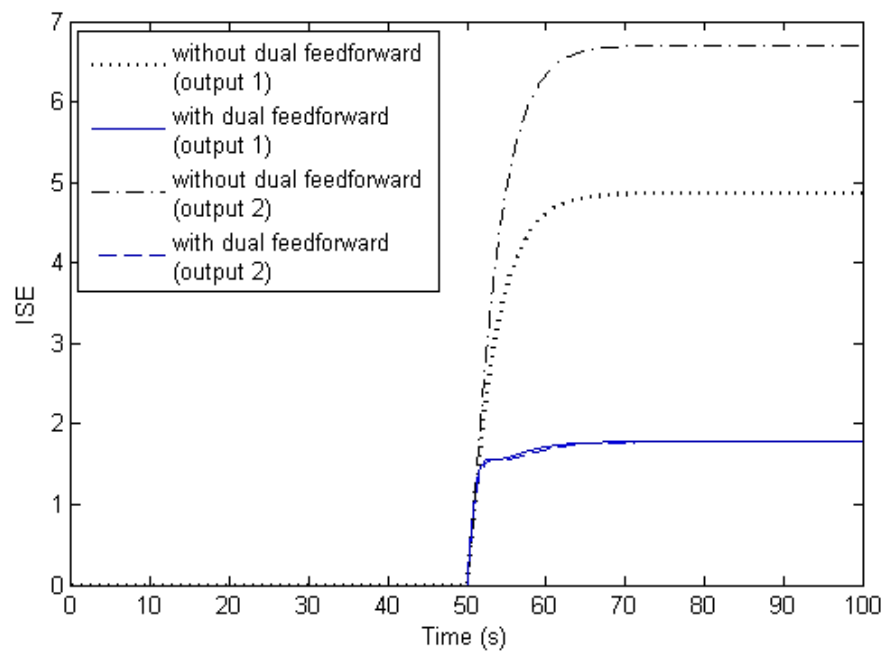


Figure 10. Closed-loop performance indices for disturbance rejection, corresponding to Example 3.

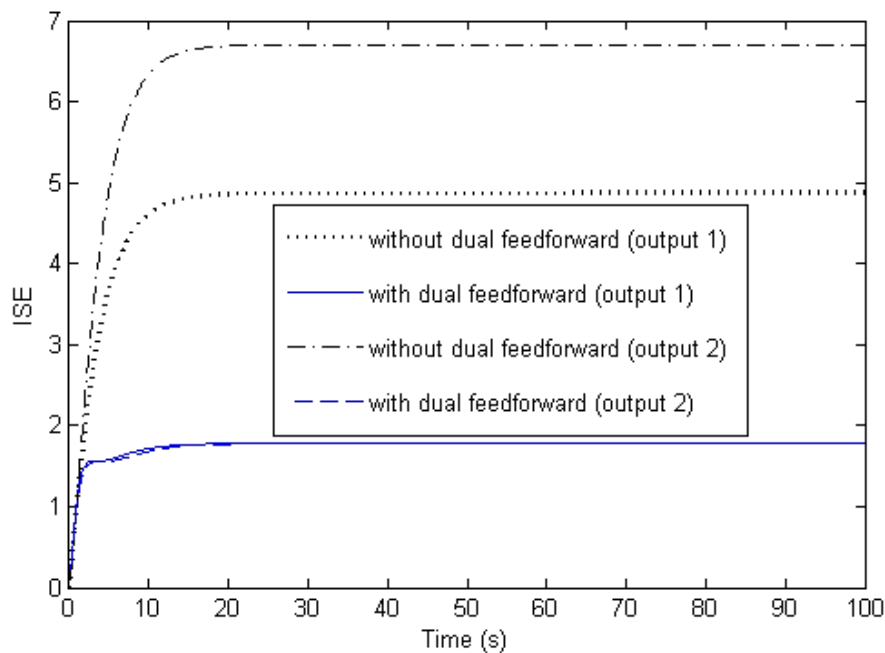


Figure 11. Closed-loop performance indices for set-point tracking, corresponding to Example 3.

Example 4: The transfer function matrix of a boiler is given as follows [28],

$$P_4(s) = \begin{bmatrix} \frac{1}{4s+1} & \frac{0.7}{5s+1} & \frac{0.3}{5s+1} & \frac{0.2}{5s+1} \\ \frac{0.6}{5s+1} & \frac{1}{4s+1} & \frac{0.4}{5s+1} & \frac{0.35}{5s+1} \\ \frac{0.35}{5s+1} & \frac{0.4}{5s+1} & \frac{1}{4s+1} & \frac{0.6}{5s+1} \\ \frac{0.2}{5s+1} & \frac{0.3}{5s+1} & \frac{0.7}{5s+1} & \frac{1}{4s+1} \end{bmatrix} \quad (33)$$

Each entry of the transfer matrix is a first-order transfer function and its dynamics is quite coupled. The controller used here is a PID controller designed using the method proposed in [16]. The matrix gains of the controller are as the following

$$K_p = \begin{bmatrix} 8.5476 & -1.0657 & -0.8035 & 0.8051 \\ 0.9150 & 8.5624 & 1.7378 & -0.3342 \\ -0.3417 & -0.2676 & 7.7622 & 0.0540 \\ -0.2844 & 1.9745 & -2.0176 & 7.9561 \end{bmatrix}, K_i = \begin{bmatrix} 1.1119 & 0.3586 & 0.1764 & 0.0187 \\ 0.1155 & 0.7111 & 0.3032 & 0.3792 \\ 0.1905 & 0.2993 & 0.9710 & 0.3687 \\ 0.1717 & 0.3016 & 0.3951 & 1.1081 \end{bmatrix}, \quad (34)$$

$$K_d = \begin{bmatrix} 0.0055 & 0.0142 & 0.0139 & -0.0080 \\ -0.0047 & -0.0043 & -0.00136 & 0.0044 \\ 0.0013 & 0.0043 & -0.0035 & 0.0003 \\ 0.0022 & -0.0122 & 0.0239 & 0.0140 \end{bmatrix}$$

The following dual-feedforward controller is also obtained using the proposed method

$$F_1(s) = F_2(s) = \begin{bmatrix} \frac{35.93s + 9.447}{s + 5.403} & \frac{-17.35s - 6.53}{s + 5.391} & \frac{-1.41s - 0.8709}{s + 5.49} & \frac{0.5767s + 0.9073}{s + 5.355} \\ \frac{-15.2s - 5.293}{s + 5.403} & \frac{37.19s + 10.11}{s + 5.391} & \frac{-5.202s - 1.267}{s + 5.49} & \frac{-2.69s - 1.723}{s + 5.355} \\ \frac{-5.588s - 1.738}{s + 5.403} & \frac{-3.355s - 1.244}{s + 5.391} & \frac{37.73s + 10.29}{s + 5.49} & \frac{-15.9s - 5.246}{s + 5.355} \\ \frac{2.868s + 0.9154}{s + 5.403} & \frac{-3.791s - 0.8551}{s + 5.391} & \frac{-17.49s - 6.65}{s + 5.49} & \frac{35.7s + 9.362}{s + 5.355} \end{bmatrix} \quad (35)$$

The step responses and control signals are shown in Figures 12 and 13, respectively. The corresponding performance indices are summarized in Tables 5 and 6. These results confirm that the dual-feedforward method acts very well in improving the disturbance rejection and set-point tracking.

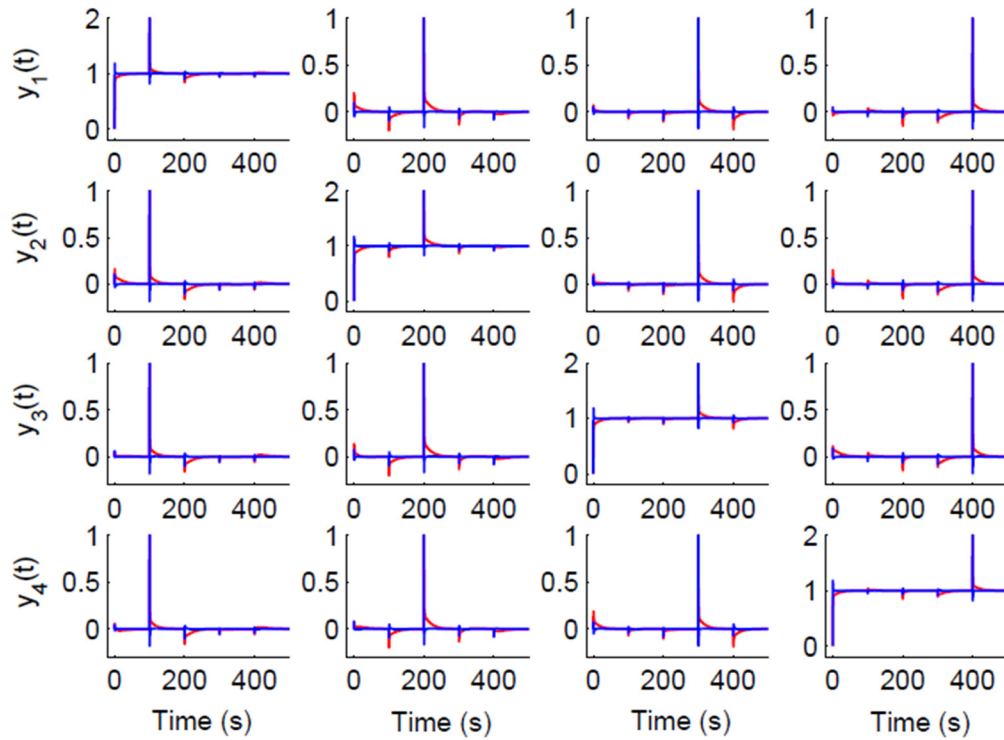


Figure 12. Comparing the closed-loop step response without (red line) and with (blue line) feedforward controller.

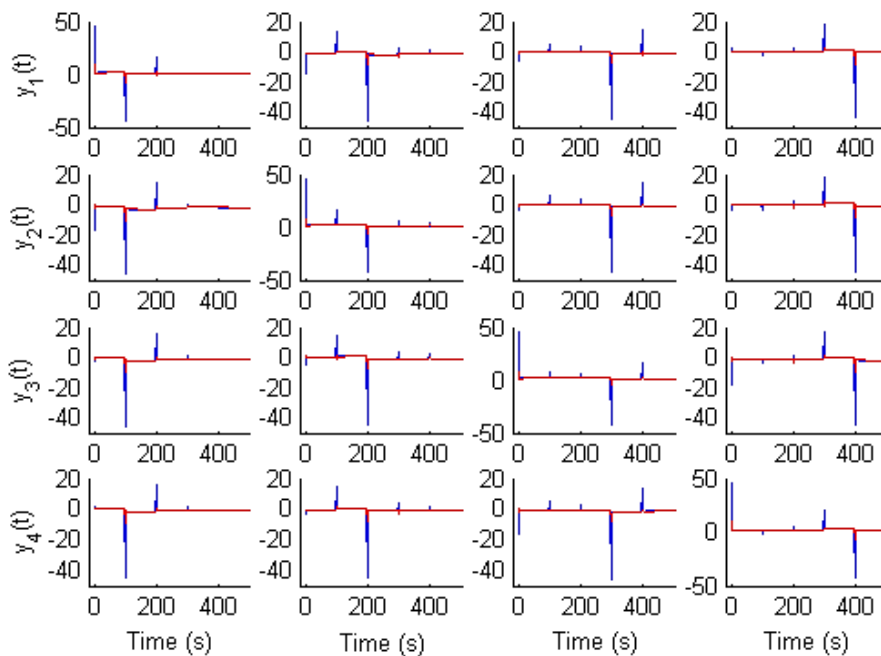


Figure 13. Control signals without (red line) and with (blue line) employing the feedforward controllers.

Table 5. Closed-loop performance indices for disturbance rejection, corresponding to Example 3.

System	Error	IAE	ISE	ITAE	ITSE
With Feedforward	e_1	0.6742	7.38×10^{-2}	127.93	0.1074×10^4
Without Feedforward	e_1	5.5429	48.45×10^{-2}	1205.89	1.1136×10^4
With Feedforward	e_2	0.8164	7.64×10^{-2}	183.85	0.3312×10^4
Without Feedforward	e_2	7.2393	71.45×10^{-2}	1698.72	3.1259×10^4
With Feedforward	e_3	0.7464	7.8×10^{-2}	229.06	0.37171×10^4
Without Feedforward	e_3	5.6917	62.89×10^{-2}	1815.58	6.4161×10^4
With Feedforward	e_4	0.7506	7.55×10^{-2}	236.65	1.1434×10^4
Without Feedforward	e_4	5.3637	51.93×10^{-2}	1778.38	2.3365×10^4

Table 6. Closed-loop performance indices for set-point tracking, corresponding to Example 3.

System	Error	IAE	ISE	ITAE	ITSE
With Feedforward	e_1	0.3371	6.73×10^{-2}	2.845	0.1107
Without Feedforward	e_1	2.201	35.65×10^{-2}	31.327	13.9219
With Feedforward	e_2	0.3935	6.68×10^{-2}	4.1519	0.2351
Without Feedforward	e_2	3.5614	55.92×10^{-2}	57.7896	48.8058
With Feedforward	e_3	0.3774	7.04×10^{-2}	3.3063	0.1628
Without Feedforward	e_3	2.8839	49.98×10^{-2}	41.3252	25.9555
With Feedforward	e_4	0.3372	6.87×10^{-2}	2.8632	0.1193
Without Feedforward	e_4	2.3726	39.17×10^{-2}	33.5154	17.0491

6. Conclusions

In this paper, we introduced a dual-feedforward controller for MIMO systems to cope with disturbances and also improve set-point tracking. The LMI approach is employed for the first time to design a MIMO feedforward controller. For this purpose, an LMI approximation is proposed for non-convex/nonlinear terms. This method is naturally iterative and the results show that it works well for the objectives under consideration. Also, in this method, a new structure for the feedforward controller is proposed. In this structure, each entry of the feedforward controller transfer matrix is considered as a first-order transfer function. This assumption simplifies the design procedure and makes it possible to formulate the problem in the form of LMIs. In the numerical simulations, we mainly focused on the different practical systems with different dimensions and orders. The simulations revealed two main facts about the proposed dual-feedforward method. First, regardless of the dimension and order of the plant, the proposed method shows satisfactory results. The second observation is that the final results exhibit a low sensitivity to the value assigned to the initial condition used in the process of designing feedforward controllers.

Conflict of interest

The authors declare there is no conflict of interest.

References

1. L. Consolini, G. Lini, A. Piazzoli, A. Visioli, Minimum-time rest-to-rest feedforward action for PID feedback MIMO systems, *IFAC Proc. Vol.*, **45** (2012), 217–222. <http://doi.org/10.3182/20120328-3-IT-3014.00037>
2. F. García-añas, J. L. Guzmán, F. Rodríguez, M. Berenguel, T. Hägglund, Experimental evaluation of feedforward tuning rules, *IFAC Proc. Vol.*, **114** (2021), 104877. <http://doi.org/10.1016/j.conengprac.2021.104877>
3. P. Roy, B. K. Roy, Dual mode adaptive fractional order PI controller with feedforward controller based on variable parameter model for quadruple tank process, *ISA Trans.*, **63** (2016), 365–376. <http://doi.org/10.1016/j.isatra.2016.03.010>
4. Y. Hamada, Flight test results of disturbance attenuation using preview feedforward compensation, *IFAC-PapersOnLine*, **50** (2017), 14188–14193. <http://doi.org/10.1016/j.ifacol.2017.08.2086>
5. D. Carnevale, S. Galeani, M. Sassano, Transient optimization in output regulation via feedforward selection and regulator state initialization, *IFAC-PapersOnLine*, **50** (2017), 2405–8963. <http://doi.org/10.1016/j.ifacol.2017.08.677>
6. W. L. Luyben, Comparison of additive and multiplicative feedforward control, *J. Process Control*, **111** (2022), 1–7. <http://doi.org/10.1016/j.jprocont.2022.01.004>
7. Y. Du, W. Cao, J. She, M. Wu, M. Fang, Disturbance rejection via feedforward compensation using an enhanced equivalent-input-disturbance approach, *J. Franklin Inst.*, **357** (2020), 10977–10996. <http://doi.org/10.1016/j.jfranklin.2020.05.052>
8. J. Wu, Y. Han, Z. Xiong, H. Ding, Servo performance improvement through iterative tuning feedforward controller with disturbance compensator, *Int. J. Mach. Tools Manuf.*, **117** (2017), 1–10. <http://doi.org/10.1016/j.ijmachtools.2017.02.002>
9. Y. Pasco, O. Robin, P. Bélanger, A. Berry, S. Rajan, Multi-input multi-output feedforward control of multi-harmonic gearbox vibrations using parallel adaptive notch filters in the principal component space, *J. Sound Vib.*, **330** (2011), 5230–5244. <http://doi.org/10.1016/j.jsv.2011.06.008>
10. S. Liu, G. Shi, D. Li, Active disturbance rejection control based on feedforward inverse system for turbofan engines, *IFAC-PapersOnLine*, **54** (2021), 376–381. <http://doi.org/10.1016/j.ifacol.2021.10.191>
11. D. Vrecko, M. Nerat, D. Vrancic, G. Dolanc, B. Dolenc, B. Pregelj, et al., Feedforward-feedback control of a solid oxide fuel cell power system, *Int. J. Hydrog. Energy*, **43** (2018), 6352–6363. <http://doi.org/10.1016/j.ijhydene.2018.01.203>
12. L. Liu, S. Tian, D. Xue, T. Zhang, Y. Q. Chen, Industrial feedforward control technology: a review, *J. Intell. Manuf.*, **30** (2019), 2819–2833. <http://doi.org/10.1007/s10845-018-1399-6>
13. M. N. A. Parlakci, E. M. Jafarov, A robust delay-dependent guaranteed cost PID multivariable output feedback controller design for time-varying delayed systems: An LMI optimization approach, *Eur. J. Control*, **61** (2021), 68–79. <http://doi.org/10.1016/j.ejcon.2021.06.003>
14. Z. Y. Feng, H. Guo, J. She, L. Xu, Weighted sensitivity design of multivariable PID controllers via a new iterative LMI approach, *J. Process Control*, **110** (2022), 24–34. <http://doi.org/10.1016/j.jprocont.2021.11.016>
15. F. Zheng, Q. G. Wang, T. H. Lee, On the design of multivariable PID controllers via LMI approach, *Automatica*, **38** (2002), 517–526. [http://doi.org/10.1016/S0005-1098\(01\)00237-0](http://doi.org/10.1016/S0005-1098(01)00237-0)

16. S. Boyd, M. Hast, K. J. Astrom, MIMO PID tuning via iterated LMI restriction, *Int. J. Robust Nonlinear Control*, **26** (2016), 1718–1731. <http://doi.org/10.1002/rnc.3376>
17. J. Sabatier, M. Moze, C. Farges, LMI stability conditions for fractional order systems, *Comput. Math. Appl.*, **59** (2010), 1594–1609. <http://doi.org/10.1016/j.camwa.2009.08.003>
18. S. Skogestad, I. Postlethwaite, *Multivariable Feedback Control: Analysis and Design*, 2nd edition, Wiley, New York, 2005.
19. C. Farges, M. Moze, J. Sabatier, Pseudo-state feedback stabilization of commensurate fractional order systems, *Automatica*, **46** (2010), 1730–1734. <http://doi.org/10.1016/j.automatica.2010.06.038>
20. Q. Tran Dinh, S. Gumussoy, W. Michiels, M. Diehl, Combining convex-concave decompositions and linearization approaches for solving BMIs, with application to static output feedback, *IEEE Trans. Autom. Control*, **57** (2011), 1377–1390. <http://doi.org/10.1109/TAC.2011.2176154>
21. S. Tofighi, F. Bayat, F. Merrikh-Bayat, Robust feedback linearization of an isothermal continuous stirred tank reactor: H_∞ mixed-sensitivity synthesis and DK-iteration approaches, *Trans. Inst. Meas. Control*, **39** (2017), 344–351. <http://doi.org/10.1177/0142331215603446>
22. *Research CVX*, CVX: Matlab software for disciplined convex programming, 2012. Available from: <http://cvxr.com/cvx> (Accessed on March 2021).
23. R. H. Tutuncu, K. C. Toh, M. J. Todd, Solving semidefinite-quadratic-linear programs using SDPT3, *Math. Program.*, **95** (2003), 189–217. <http://doi.org/10.1007/s10107-002-0347-5>
24. R. Wood, M. Berry, Terminal composition control of a binary distillation column, *Chem. Eng. Sci.*, **28** (1973), 1707–1717. [http://doi.org/10.1016/0009-2509\(73\)80025-9](http://doi.org/10.1016/0009-2509(73)80025-9)
25. M. Hovd, M. Skogestad, Simple frequency tools for control system analysis, structure selection and design, *Automatica*, **28** (1992), 989–996. [http://doi.org/10.1016/0005-1098\(92\)90152-6](http://doi.org/10.1016/0005-1098(92)90152-6)
26. F. Merrikh-Bayat, An iterative LMI approach for H_∞ synthesis of multivariable PI/PD controllers for stable and unstable processes, *Chem. Eng. Res. Des.*, **132** (2018), 606–615. <http://doi.org/10.1016/j.cherd.2018.02.012>
27. S. Tofighi, F. Merrikh-Bayat, A benchmark system to investigate the non-minimum phase behaviour of multi-input multi-output systems, *J. Control Decis.*, **5** (2018), 300–317. <http://doi.org/10.1080/23307706.2017.1371653>
28. H. H. Rosenbrock, *Computer-Aided Control System Design*, Academic Press, New York, 1974.



AIMS Press

©2022 the Author(s), licensee AIMS Press. This is an open access article distributed under the terms of the Creative Commons Attribution License (<http://creativecommons.org/licenses/by/4.0>)